CHAPTER 7

APPLICATION OF PRESENT MODEL TO STONE PROCESSING ZONE IN SARABURI

The fugitive dust with diameter less than 10 micrometer (PM_{10}) from numerous stone processing plants affects the air quality in Saraburi province, which abounds with superior limestone sources clustered in Thumbol Na Pra Laan and the vicinity. At present, over 45 stone processing plants located in Na Pra Laan and vicinity contribute to the high ambient particulate concentration with fugitive dust from their processes and the transportation of final products.

7.1 Description of Case Study

To find out the condition causing an excessively high ambient PM_{10} concentration, the predicted 24-hr-averaged PM_{10} concentration above the ground level is used to indicate the effect of the significant factors. The interested area in Thumbol Na Pra Laan covers an area of about 45 square kilometers in which over a population of 70,000 live. The topographical contours of the area, actual source or plant locations and selected receptor positions are shown in Figure 7.1. Though in reality there is only one single monitoring station for the ambient PM_{10} concentration belonging to Department of Pollution Control, Ministry of Science, Technology and Environment, Thailand, a variety of receptor points are selected in the simulation. Since the values of all model inputs (e.g. wind speed and direction) and parameters (e.g. horizontal and vertical dispersion coefficients) are not allowed to vary with time during each simulation run, and since the initial values of the PM_{10} at the start of each simulation are arbitrarily set as zero, it is decided to focus on the 1-hr-averaged concentration observed after the system

has approached a steady state. From Figure 7.2, it is obvious that by the third hour the system has become steady.

As discussed in Chapter 6, besides wind direction and wind speed, the atmospheric stability is one of the most important factors affecting the predicted air pollutant concentration in mountainous area, while the vertical dispersion coefficient inversely reflects the stability level. A low vertical dispersion coefficient will result from an increase in the stability of the atmospheric condition. In this chapter, effects of wind direction, wind speed and vertical dispersion coefficient will be discussed. First, wind direction and speed data collected by Pollution Control Department at Na Pra Laan receptor point during January-March, 2000 are used to analyze for the prevalent wind direction and speed in the area. During the said period, it is found that the prevalent wind direction and speed are in the ranges of 180-225 degrees and 0-1.5 m/s, respectively, as shown in Figure 3.11. The stability class of the area and the mixing height are discussed in the section 7.1.1 and 7.1.2

7.1.1 Atmospheric Stability

The frequency of occurrence of the stability class in the study area during January-March, 2000 is shown in Figure G.1 of Appendix G. The symbols A, B, C, D, E, and F classes mean, respectively, extremely unstable, moderately unstable, slightly unstable, neutral, slightly stable, and moderately stable classes. From Figure G.1, it is seen that most of the atmospheric stability class of the study area is moderately stable or F class. In the case of the stable atmospheric condition, the horizontal dispersion coefficient and vertical dispersion coefficient may be assigned the values of 200 and 1 m^2/s, respectively, as recommended by Prof. Y.Takemoto(1997).

7.1.2. Mixing Height

Because there is no mixing height data in the area of study, the mixing height data of Bangkok is used to represent that of Saraburi. From historical

mixing height data observed at the monitoring station of Thailand Meteorological Department in Bangkok from January 2000 to March 2000, the average mixing height is 1,022 m above the ground. So, in this study the height of the simulated study area covers 1,000 m above the ground. Anyway, because the heights of most of the sources and receptors is just 10 m above the ground, the effect of the mixing height is comparatively insignificant when compared with the others. By the way, the mixing height data of the area during January-March, 2000, is given in the Appendix G.

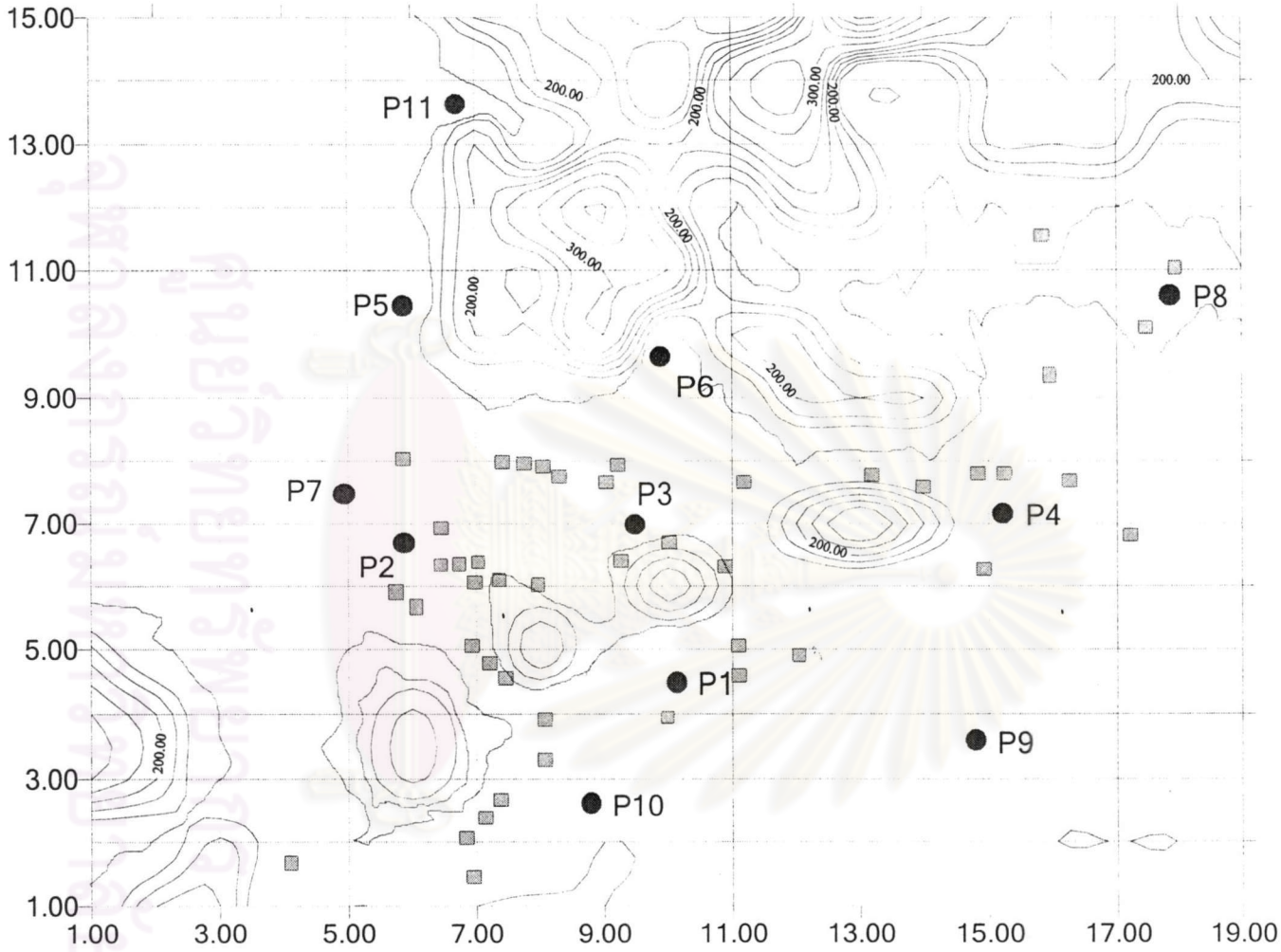

Figure 7.1 Map of the study area with locations of stone-processing plants (square dots) and receptors (round dots)

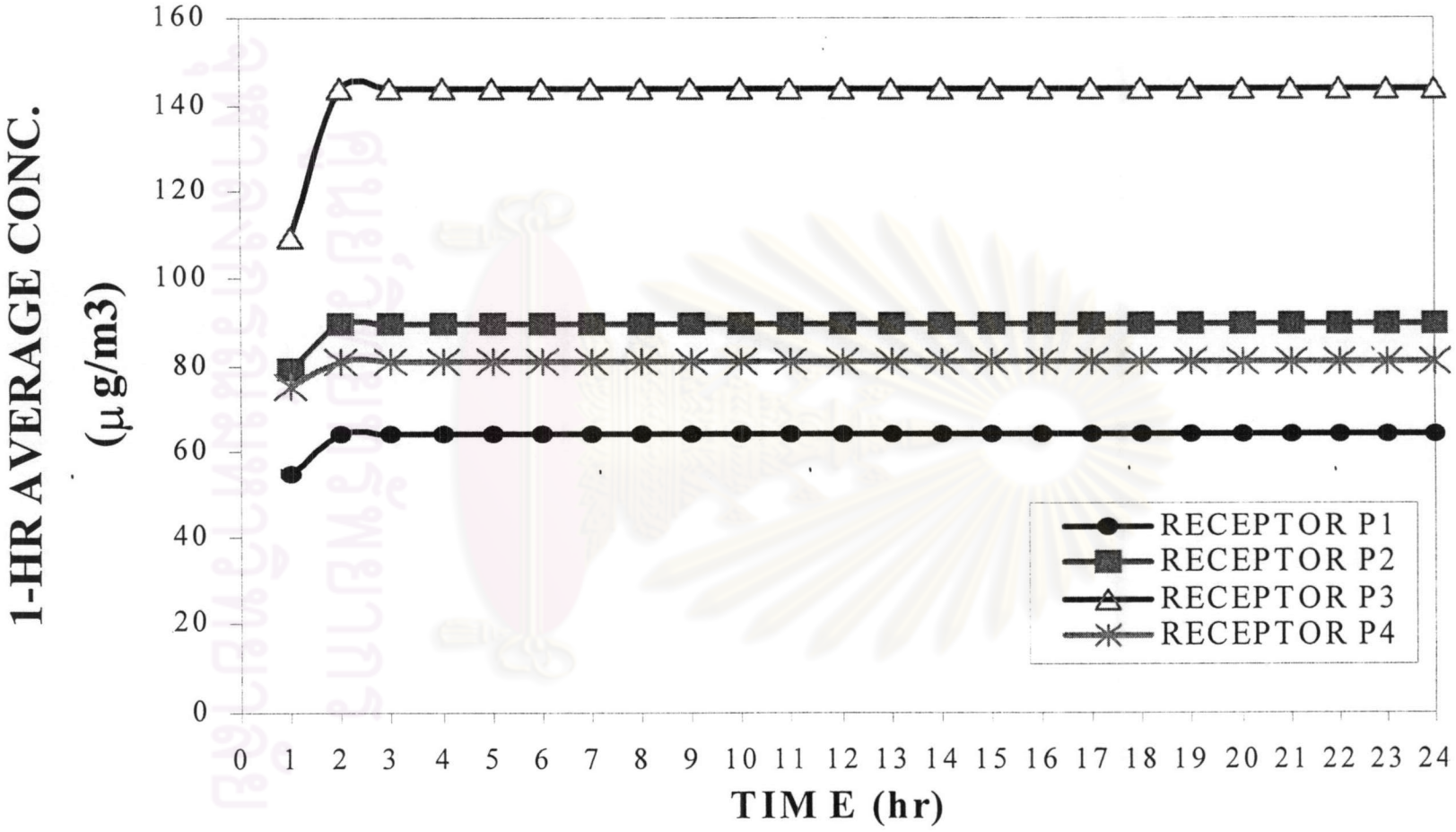

Figure 7.2 The predicted 1-hr-averaged concentration vs. simulation time at various receptors

7.2 Additional assumptions used in the present case study

In addition to the assumptions used in the development of the model, the additional assumptions are as follows:

1. In the study, each stone crushing plant is assumed to be equivalent to a point source.

2. The equivalent stack height, or release height, of each point source is assumed to be about 10 meter above the ground, which is about a half of the typical height of the stone-crushing plant. The dimensions of the surveyed typical stone-processing plant (Meechumna, P., et al., 1999) where the main crushing process occurs are shown in Appendix F.

3. As for the fugitive dust emission, it is assumed that the released plume has essentially the same temperature as ambient air because there is negligible plume rise during the crushing process.

4. In this study, the dust emission rate of each source is estimated as the multiplication product between a suitable emission factor and the plant production capacity. The emission factor of PM_{10} used in this work was taken from the U.S. EPA AP-42 document. In Table E.11, the U.S. EPA emission factors for PM_{10} with and without any dust control system are presented. An example of the calculation of the emission rate for the stone-processing plants is shown in Appendix E.

7.3 Evaluation of input parameters of the model

In order to evaluate the suitability of the values of the parameters of the model, i.e. Reynolds number of 1000, the exponent of the power law of 0.55, the horizontal dispersion coefficient of 200 m^2/s and the vertical dispersion coefficient of 1 m^2/s as well as emission factor of 0.5275 are used along with the assumption that there were ineffective or no dust suppression systems in use. Figure G.2 of Appendix G compares the 1-hr average ambient concentration of PM_{10} predicted by the model at the receptor height of 10 meter

above the ground with its counterpart concentration measured at the monitoring station in Na Pra Laan area during January 6-12, 2000. Figure G.3 of Appendix G compares the 24-hr-average ambient concentration of PM_{10} predicted by the model at the receptor height of 10 meter above the ground with its counterpart concentration measured at the monitoring station in Na Pra Laan area during January 6-12, 2000.

In Figure G.2, the predicted 1-hr predicted average concentration of PM10 from the model is found to exhibit significant deviation from the measured data due to the fluctuation in wind speed and direction as well as the dispersion of fugitive PM_{10} from activities other than the stone crushing activity. Nevertheless, the predicted 24-hr predicted average concentration of PM_{10} agree with the measured data as shown in Figure G.3. Consequently, these parameters are reliable for the prediction of ambient PM_{10} concentration during the selected time.

According to the change in the actual atmospheric stability, wind speed and wind direction as well as other meteorological data, the change in the predicted PM_{10} concentration caused by a shift in the factors i.e. wind speed, wind direction and atmospheric stability from the prevalent values of during the January-March 2000 is studied. As a result, in this chapter, the ranges of wind direction, wind speed and vertical dispersion coefficient as well as the simulation conditions used to investigate the effect of these factors are as shown in Tables 7.1and 7.2, respectively.

Table 7.1 Maximum and minimum values of main factors investigated

Range	Main factor		
	K_V (m^2/s)	WD (degrees)	E = WS (m/s)
Minimum	1	179	0.5
Maximum	10	239	2

Note that the wind speeds specified in Table 7.1 are at a height of 10 meter above the ground.

Table 7.2 Simulation conditions used to investigate the effects of the significant factors

Simulation condition	
Number of grid points in the x, y and z directions	19 x 21 x 15
Grid size ($\Delta x, \Delta y, \Delta z$)	500, 50, 500 m.
Reynolds no.	1000
Exponent of the power law	0.55
Integration step size(Δt)	0.25 sec.

In section 7.3, the simulated effects of the factors on receptors P1, P2, P3, P4, P6 and P8 will be discussed.

7.4 Boundary conditions of the model

As for the boundary conditions of the model, they are set in 2 step as follows:

For wind profile calculation:

-On the ground surface (plane j=1), all u, v, and w in both the physical and transformed spaces are zero.

-At plane j = jmax, u and w in the physical space are estimated by the power law and the vertical component v is assigned to be zero.

-At planes i=1 and imax , u and w in the physical space are also those estimated by the power law and v is also zero.

-At planes k=1 and kmax , u and w in the physical space are also those estimated by the power law and v is also zero.

At planes i=1, i= imax, k=1, and k= kmax, the air pressure is assigned to atmospheric pressure and the air temperature is 30 °C.

The boundary conditions for the concentration are as follows:

- $C = 0$, at $x = -\frac{\Delta x}{2}$ (0<z<zmax, 0<y<ymax)

- $C = 0$, at $x = x_{max} + \frac{\Delta x}{2}$ (0<z<zmax, 0<y<ymax)

- $C = 0$, at $z = -\frac{\Delta z}{2}$ (0<x<xmax, 0<y<ymax)

- $C = 0$, at $z = z_{max} + \frac{\Delta z}{2}$ (0<x<xmax, 0<y<ymax)

- $C = 0$, at $y = -\frac{\Delta y}{2}$ (0<x<xmax, 0<z<zmax)

- $C = 0$, at $y = y_{max} + \frac{\Delta y}{2}$ (0<x<xmax, 0<z<zmax)

-The fugitive PM_{10} is assumed to be released from each plant as a point source which appears in the multiple-source term as Q in equation.4.5.

7.5 Effects of changes in significant factors on the predicted 1-hour concentration at receptor points

The effects of wind direction, wind speed and vertical dispersion coefficient and their interactions on the predicted 1-hr-averaged PM_{10} concentration at the receptor points of interest especially P1, P2, P3, and P4, are discussed in this section. The combinations of the values used in all simulation cases are listed in Table 7.3. In this study, wind directions of 239, 225, 209, and 179 degrees from the north are displayed as wind directions of 59, 45, 29 and –1 degrees with respect to zero direction or from the south, respectively. For the sake of brevity, the change in the horizontal dispersion

coefficient and one of the other factors, wind direction, speed or vertical dispersion coefficient are given in Appendix F.

Table 7.3 Values of the factors used to investigate the predicted 1-hr-averaged PM_{10} concentration at various receptor points.

Case	Horizontal dispersion coefficient (m^2/s)	Vertical dispersion coefficient (m^2/s)	Wind direction (degrees)	Wind speed (m/s)
WD-Effect	200	1	-1	1
	200	1	29	1
	200	1	45	1
	200	1	59	1
WS-Effect	200	1	29	0.25
	200	1	29	0.5
	200	1	29	1
	200	1	29	2
K_V-Effect	200	1	29	1
	200	2	29	1
	200	3	29	1
	200	4	29	1
	200	5	29	1
	200	10	29	1
K_H-Effect	20	1	29	0.5
	50	1	29	0.5
	100	1	29	0.5
	150	1	29	0.5
	200	1	29	0.5
WD&WS-Effect	200	1	29	0.25
	200	1	29	0.5
	200	1	29	1
	200	1	29	2

Table 7.3 (Cont.) Values of the factors used to investigate the predicted 1-hr-averaged PM_{10} concentration at various receptor points.

Case	Horizontal dispersion coefficient (m^2/s)	Vertical dispersion coefficient (m^2/s)	Wind direction (degrees)	Wind speed (m/s)
WD&WS-Effect	200	1	45	0.25
	200	1	45	0.5
	200	1	45	1
	200	1	45	2
WD&WS-Effect	200	1	59	0.25
	200	1	59	0.5
	200	1	59	1
	200	1	59	2
WD&K_V-Effect	200	1	-1	1
	200	2	-1	1
	200	3	-1	1
	200	4	-1	1
	200	5	-1	1
	200	10	-1	1
	200	1	29	1
	200	2	29	1
	200	3	29	1
	200	4	29	1
	200	5	29	1
	200	10	29	1
	200	1	45	1
	200	2	45	1
	200	3	45	1
	200	4	45	1
	200	5	45	1
	200	10	45	1

Table 7.3 (Cont.) Values of the factors used to investigate the predicted 1-hr-averaged PM_{10} concentration at various receptor points.

Case	Horizontal dispersion coefficient (m^2/s)	Vertical dispersion coefficient (m^2/s)	Wind direction (degrees)	Wind speed (m/s)
WD&K_V-Effect	200	1	59	1
	200	2	59	1
	200	3	59	1
	200	4	59	1
	200	5	59	1
	200	10	59	1
WS&K_V-Effect	200	1	29	0.5
	200	2	29	0.5
	200	3	29	0.5
	200	4	29	0.5
	200	5	29	0.5
	200	10	29	0.5
	200	1	29	1
	200	2	29	1
	200	3	29	1
	200	4	29	1
	200	5	29	1
	200	10	29	1
	200	1	29	2
	200	2	29	2
	200	3	29	2
	200	4	29	2
	200	5	29	2
	200	10	29	2

Table 7.3 (Cont.) Values of the factors used to investigate the predicted 1-hr-averaged PM_{10} concentration at various receptor points.

Case	Horizontal dispersion coefficient (m^2/s)	Vertical dispersion coefficient (m^2/s)	Wind direction (degrees)	Wind speed (m/s)
WD&K_H-Effect	20	1	29	0.5
	50	1	29	0.5
	100	1	29	0.5
	150	1	29	0.5
	200	1	29	0.5
	20	1	45	0.5
	50	1	45	0.5
	100	1	45	0.5
	150	1	45	0.5
	200	1	45	0.5
	20	1	59	0.5
	50	1	59	0.5
	100	1	59	0.5
	150	1	59	0.5
	200	1	59	0.5
WS&K_H-Effect	20	1	29	0.5
	50	1	29	0.5
	100	1	29	0.5
	150	1	29	0.5
	200	1	29	0.5
	20	1	29	1
	50	1	29	1
	100	1	29	1
	150	1	29	1
	200	1	29	1

Table 7.3 (Cont.) Values of the factors used to investigate the predicted 1-hr-averaged PM_{10} concentraion at various receptor points.

Case	Horizontal dispersion coefficient (m^2/s)	Vertical dispersion coefficient (m^2/s)	Wind direction (degrees)	Wind speed (m/s)
	20	1	29	2
	50	1	29	2
	100	1	29	2
	150	1	29	2
	200	1	29	2
E.F.-Effect	200	1	29	1

7.5.1 Change in wind direction

Figure 7.3 illustrates that shifting the wind direction increases the predicted average concentration at receptor P1 since the cluster of stone processing plants in the southwest direction of P1 shows a more direct by downwind effect as the wind direction shifts from –1 to 59 degrees. It is should be noted the area where those plants are located has relatively small difference in height. So the effect of the terrain when the wind direction is smaller than 45 degrees is less than when the wind direction is higher. In fact, for the wind direction in the range of 45-59 degrees, the predicted average concentration appears to be highest. Consequently, the most significant wind direction for receptor P1 lies in the range of 45-59 degrees. Similar to receptor P1, the predicted average concentration at receptor P2 rapidly increases as the wind direction shifts away from the south. From Figure 7.4, the most significant wind direction may be more than 60 degrees with respect to the south, since the receptor location lies to the north of the stone processing plants. In contrast Figure 7.5 shows the predicted average concentration at receptor P3 drops significantly from 190 to 80 $\mu g/m^3$ as the wind direction shifts from –1 to 59 degrees with respect to the south. For wind direction of –1 degrees the fugitive PM_{10} from the stone processing plants is transported more directly to receptor P_3 than the other wind directions. As shown in Figure 7.6, the wind direction slightly affects the predicted average concentration at receptor P4. This implies that in the range of wind direction investigated the ambient PM_{10} at receptor P4 is affected more by the dispersion mechanism than the convection mechanism.

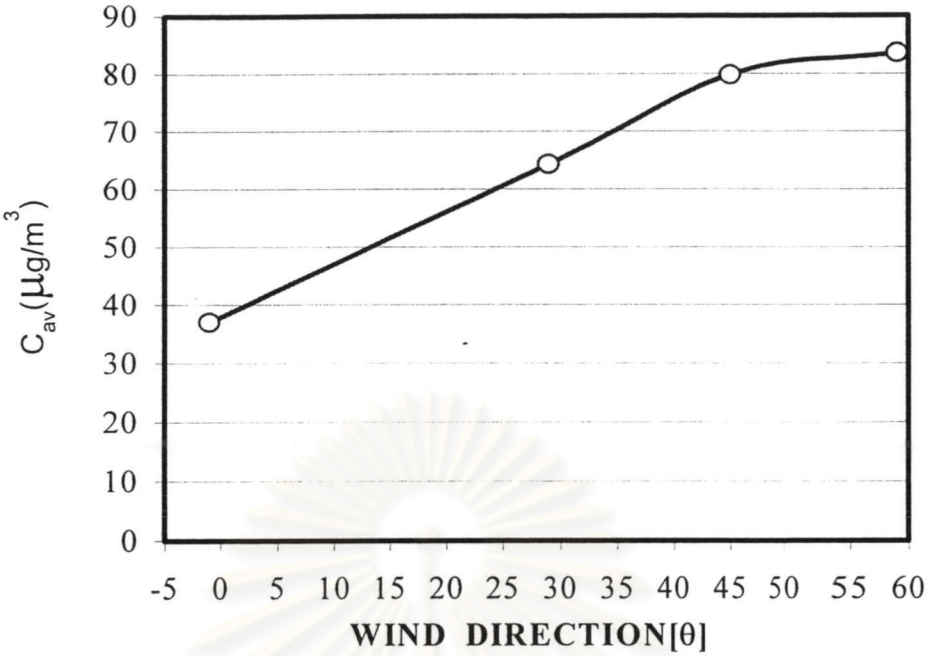

Figure 7.3 The change in predicted average concentration at Receptor P1 by the shift of wind direction

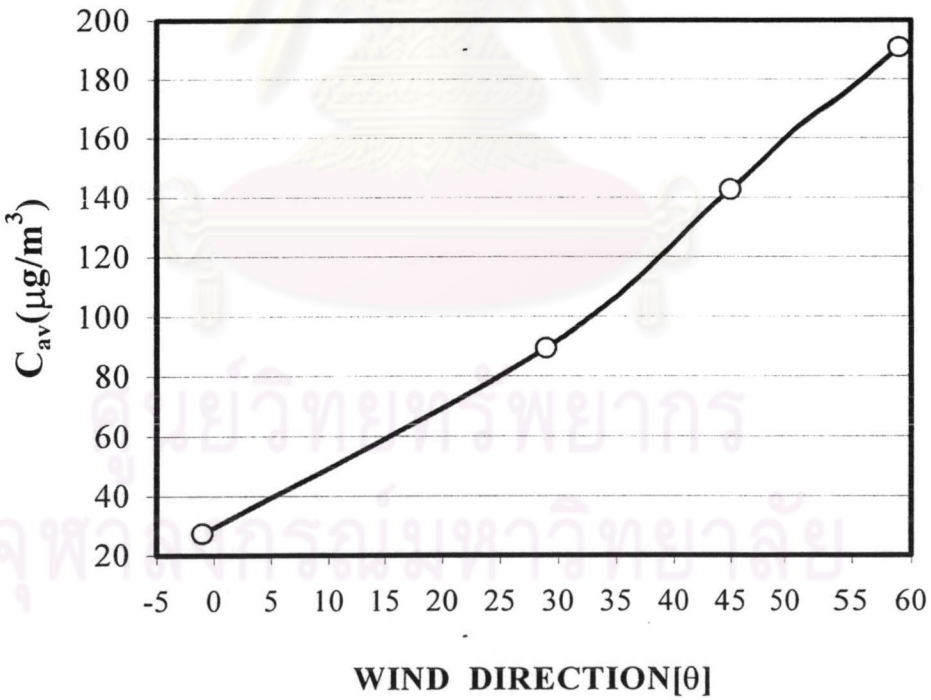

Figure 7.4 The change in predicted average concentration at Receptor P2 by the shift of wind direction

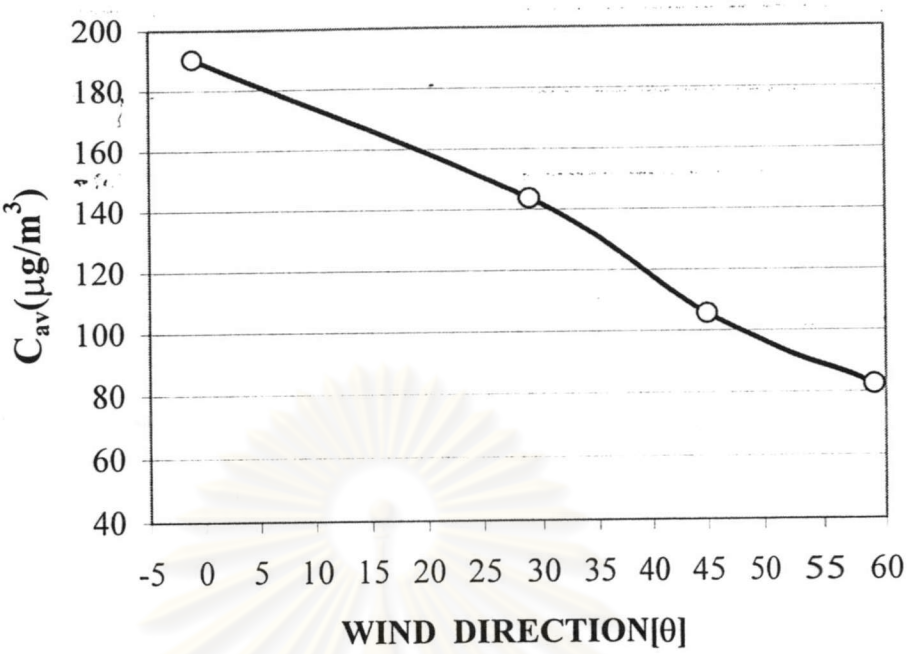

Figure 7. The change in predicted average concentration at Receptor P3 by the shift of wind direction

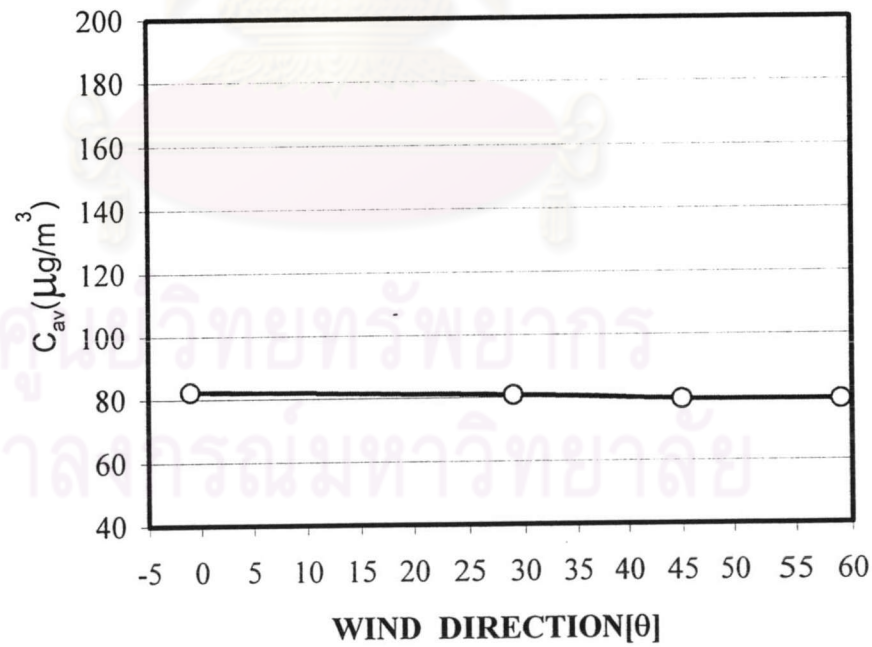

Figure 7.6 The change in predicted average concentration at Receptor P4 by the shift of wind direction

7.5.2 Change in wind speed

Figure 7.7 illustrates that the predicted average PM_{10}concentration at receptor P1 decreases by less than 10 $\mu g/m^3$ as the wind speed increases to 2 m/s. In contrast, the increasing wind speed dramatically decreases the predicted average concentration at receptor P2, as shown in Figure 7.8. So does it at receptor P4 in Figure 7.10. Meanwhile, the predicted average concentration at receptor P3 in Figure 7.9 substantially increases from 110 to 190 $\mu g/m^3$. In the case of wind direction of 29 degrees, fugitive PM_{10} from the cluster of stone processing plants is directly transported to receptor P3 because of its location. As expected, a higher wind speed tapers the PM_{10} plume width, so the concentration at P_3 along the main flow increases. However, P1, P2, and P4 are not located directly in the downwind path of the PM_{10} plume dispersing from the stone processing plants.

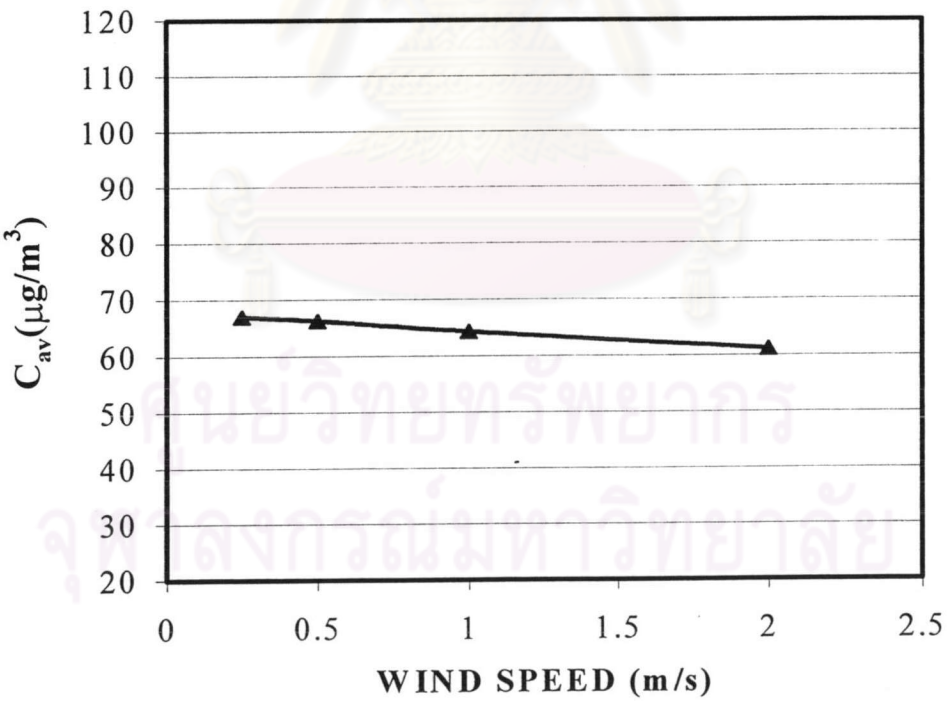

Figure 7.7 The change in predicted average concentration at Receptor P1 by the change in wind speed (wind direction 29 degrees)

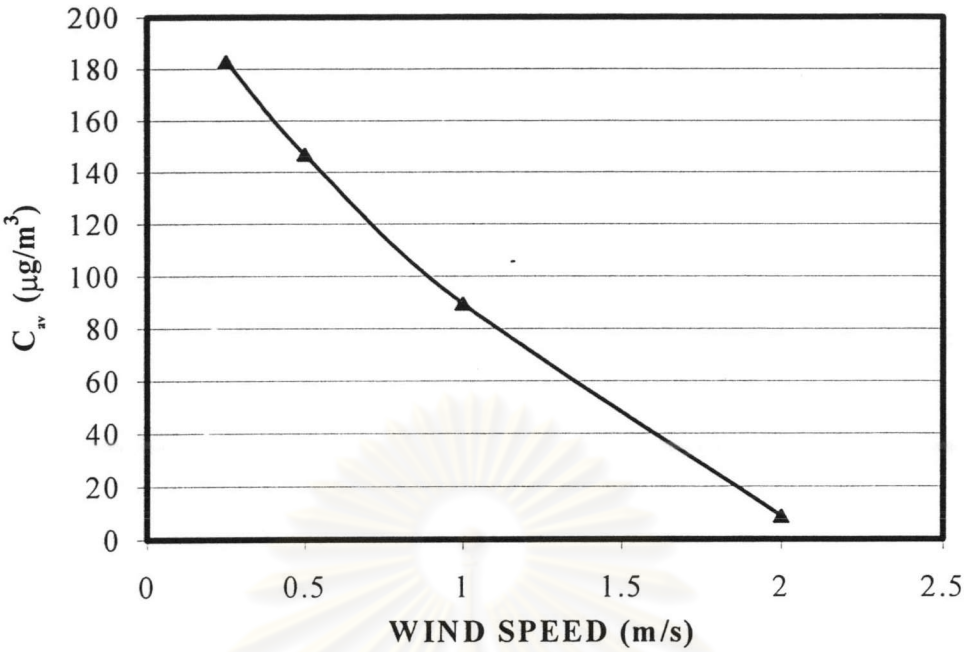

Figure 7.8 The change in predicted average concentration at Receptor P2 by the change in wind speed (wind direction 29 degrees)

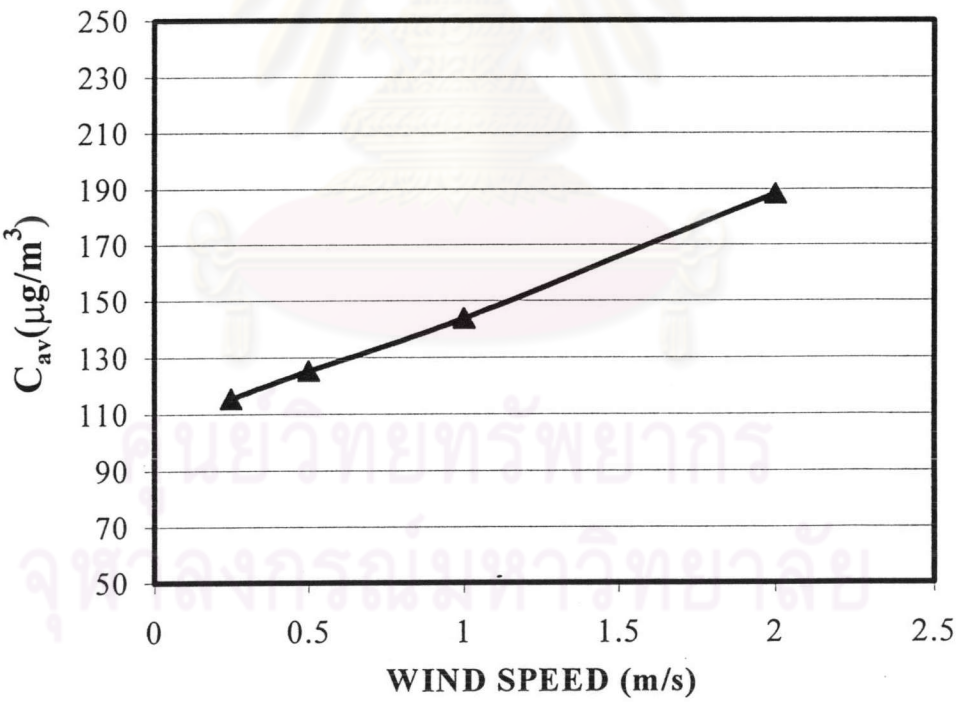

Figure 7.9 The change in predicted average concentration at Receptor P3 by the change in wind speed (wind direction 29 degrees)

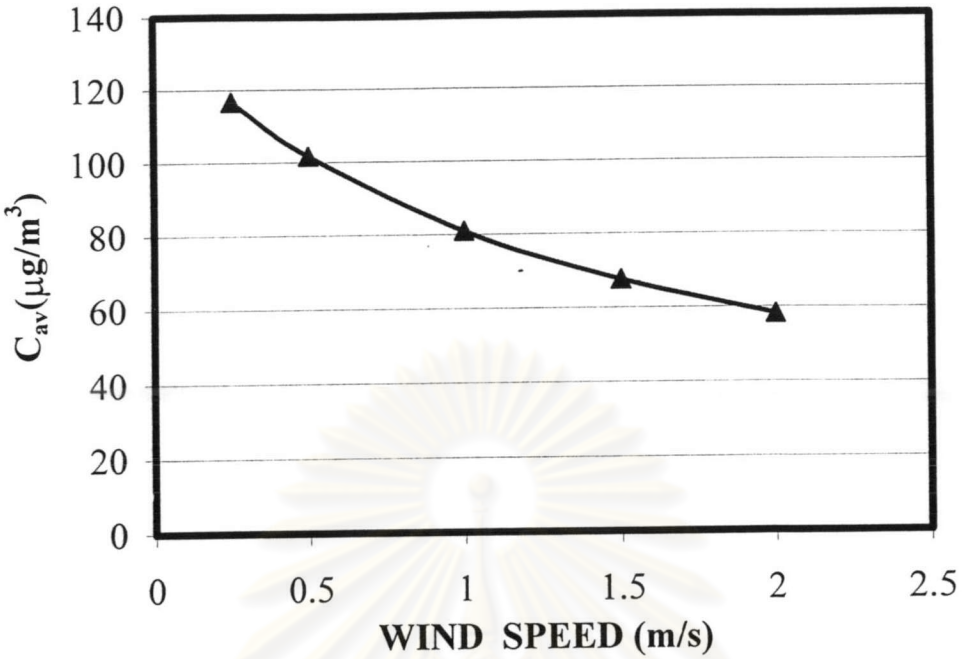

Figure 7.10 The change in predicted average concentration at Receptor P4 by the change in wind speed (wind direction 29 degrees)

7.5.3 Change in the vertical dispersion coefficient

Figures 7.11 to 7.14 reveal that an increase in the vertical dispersion coefficient seems to dramatically decrease the predicted average concentration at receptors P1, P2, P3 and P4. The predicted average concentration drops from 65 to 10 $\mu g/m^3$, from 90 to 10 $\mu g/m^3$, from 140 to 20 $\mu g/m^3$ and from 80 to 35 $\mu g/m^3$ at receptors P1, P2, P3 and P4, respectively. As mentioned before, the vertical dispersion coefficient inversely reflects the level of stability of atmospheric condition. As a result, it can be concluded that the higher the vertical dispersion coefficient, the less stable the atmospheric stability, and the lower the predicted average concentration at all receptors of interest located 10 m above the ground.

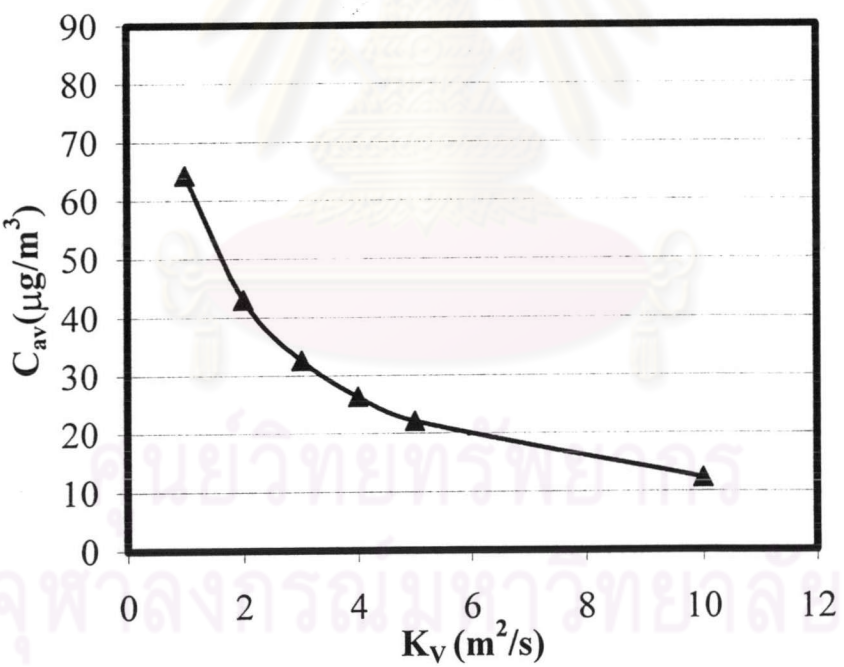

Figure 7.11 The change in the predicted average concentration at Receptor P1 by change in the vertical dispersion coefficient (K_V) (wind direction 29 degrees and wind speed 1 m/s)

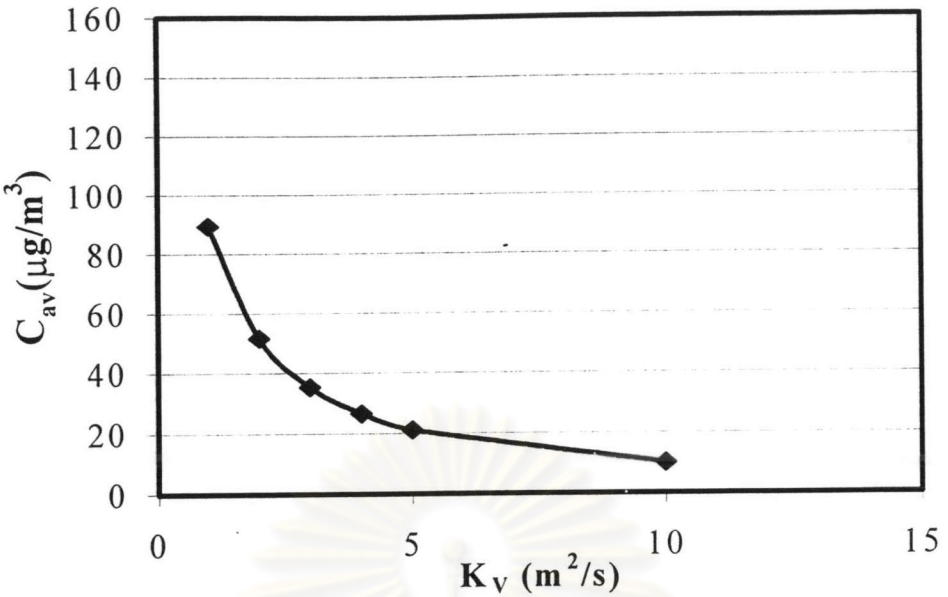

Figure 7.12 The change in the predicted average concentration at Receptor P2 by change in the vertical dispersion coefficient (K_V) (wind direction 29 degrees and wind speed 1 m/s)

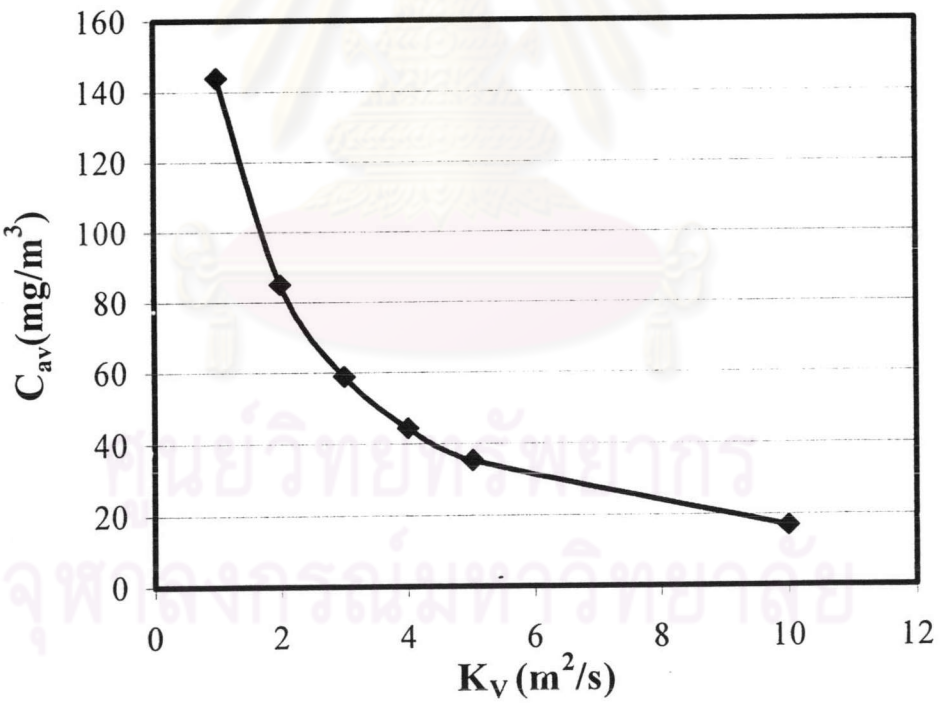

Figure 7.13 The change in the predicted average concentration at Receptor P3 by change in the vertical dispersion coefficient (K_V) (wind direction 29 degrees and wind speed 1 m/s)

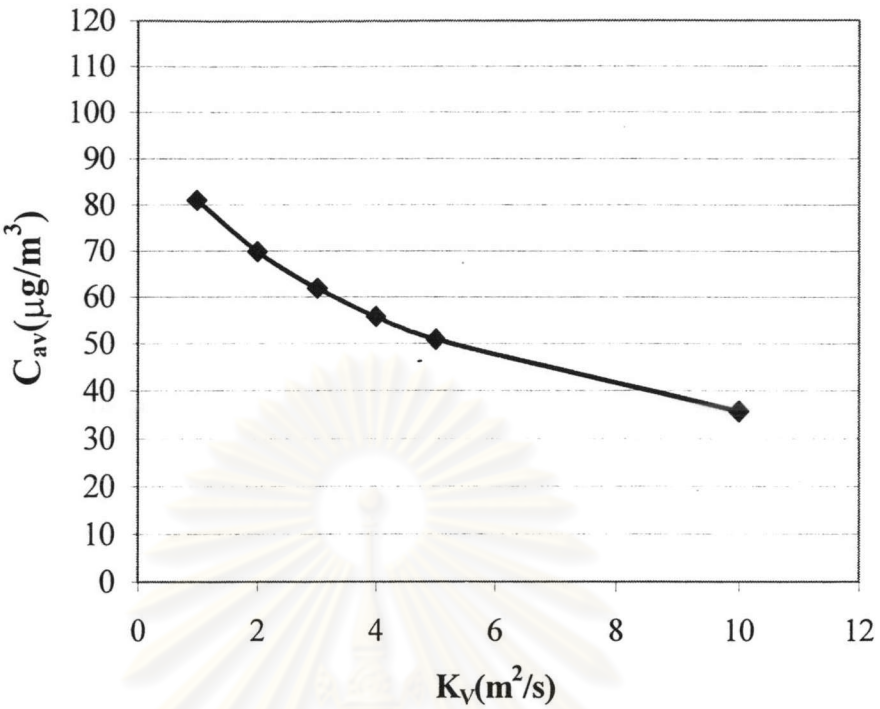

Figure 7.14 The change in the predicted average concentration at Receptor P4 by change in the vertical dispersion coefficient (K_V) (wind direction 29 degrees and wind speed 1 m/s)

7.5.4 Change in wind direction and wind speed

From the discussion of the individual change in wind direction in section 7.5.1, the most significant wind direction for receptor P1 is in the range of 45 and 59 degrees. Figure 7.15 illustrates that for wind direction of 59 degrees the predicted average concentration tends to stabilize at wind speed higher than 2 m/s whereas for wind direction of 45 degrees, the predicted average concentration tends to increase at wind speed higher than 2 m/s. In case of wind direction of 29 degrees, increasing the wind speed decreases the predicted average concentration because in this wind direction the spread of the fugitive dust to the receptor depends on the dispersion mechanism more than the convection mechanism. This is because the locations of major stone processing plants affecting the concentration at receptor P1 all lie in the southeast of the receptor.

In Figure 7.16, for all wind directions, the predicted average concentration at receptor P2 rapidly decreases as the wind speed increases, since the wind in the all wind directions flows away from receptor P_2. As for receptor P3, the predicted average concentration rapidly increases in wind direction of 29 degrees, slightly drops in wind direction of 59 degrees and seems to stabilize in wind direction of 45 degrees, as shown in Figure 7.17, because of its location. Figure 7.18 shows that at receptor P4, only the wind speed has a negative effect on the predicted average concentration, whereas the wind direction hardly has any effect.

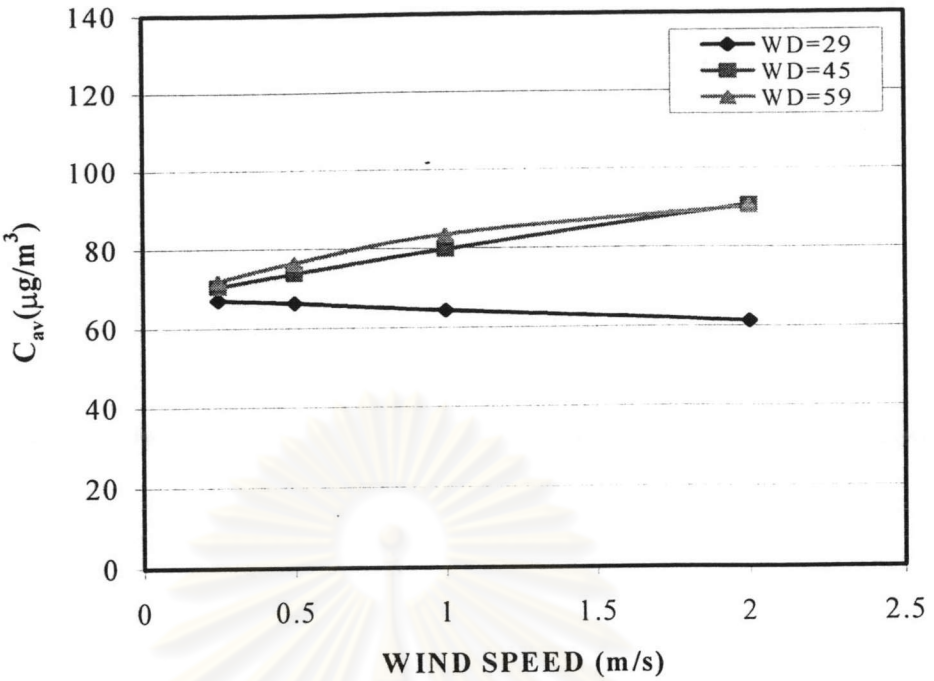

Figure 7.15 The change in the predicted average concentration at Receptor P1 by the change in wind speed (WS) at various wind directions

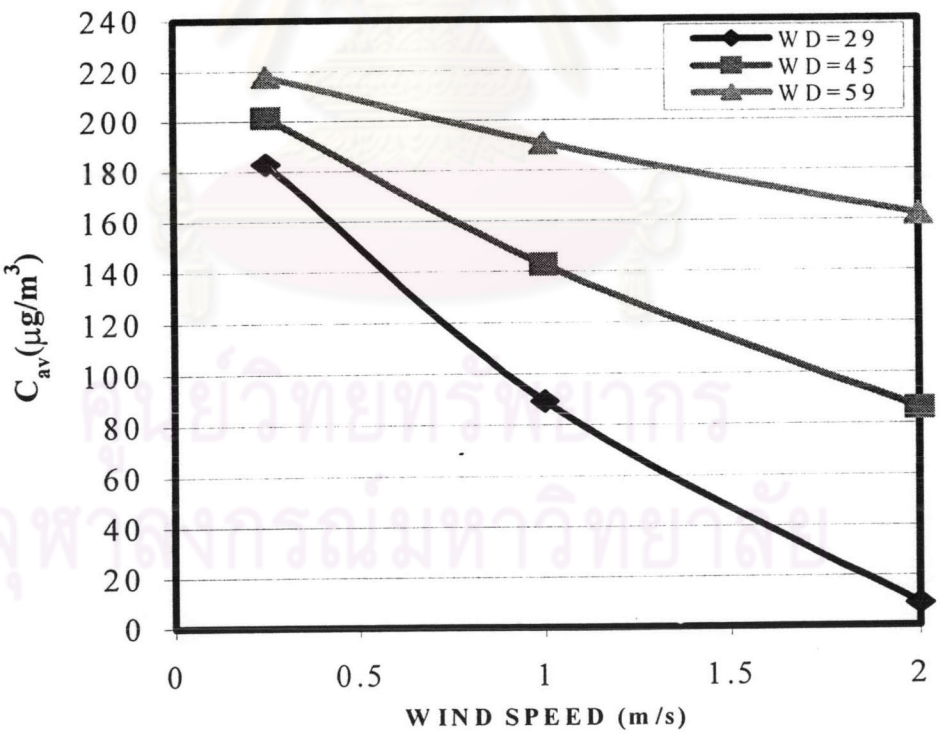

Figure 7.16 The change in the predicted average concentration at Receptor P2 by the change in wind speed (WS) at various wind directions

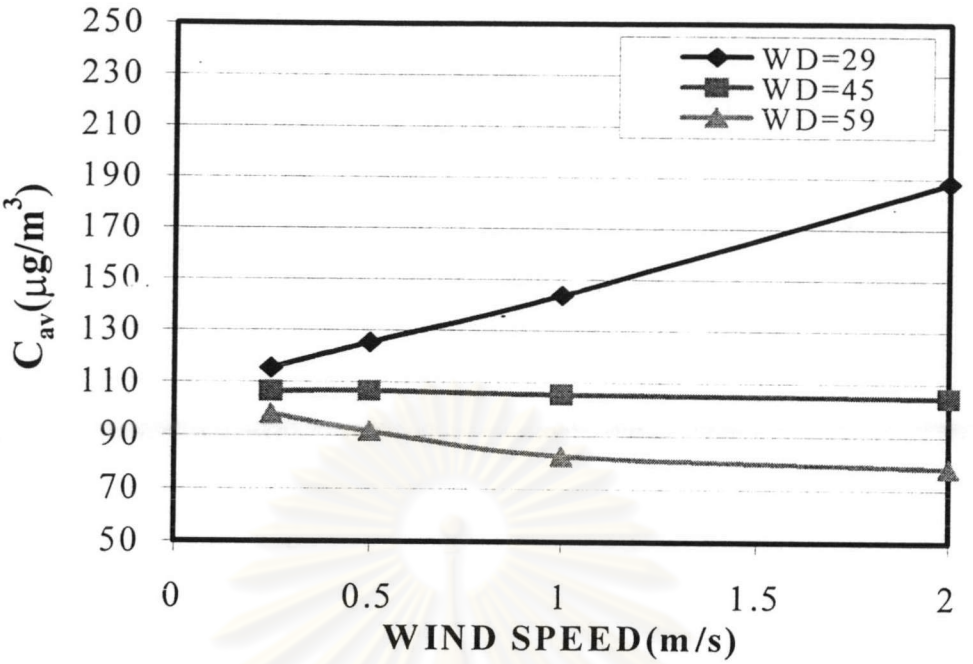

Figure 7.17 The change in the predicted average concentration at Receptor P3 by the change in wind speed (WS) at various wind directions

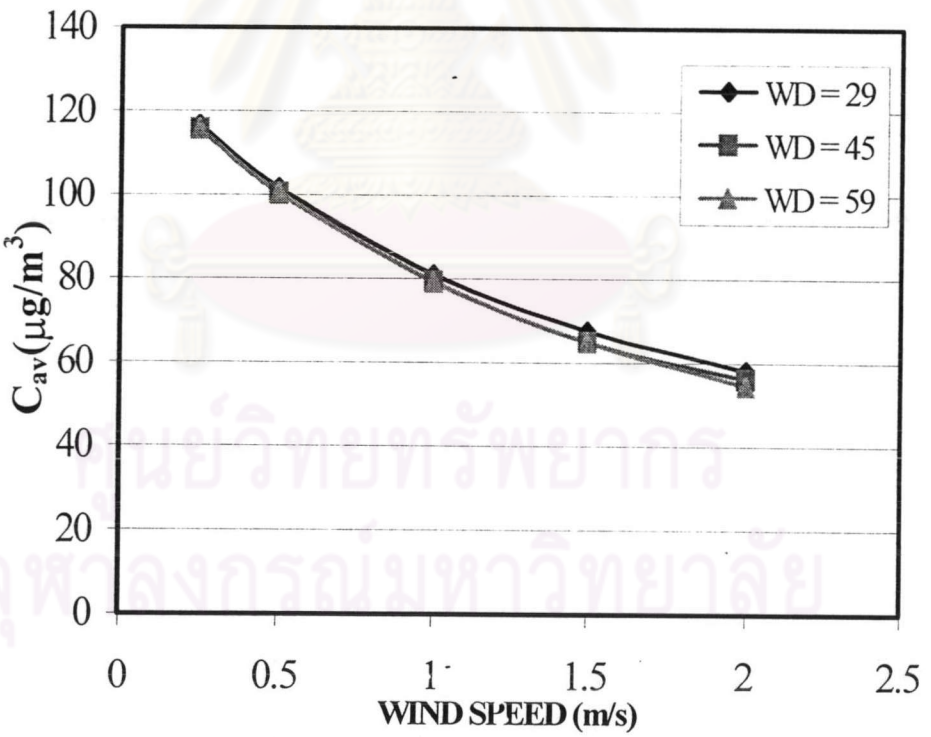

Figure 7.18 The change in the predicted average concentration at Receptor P4 by the change in wind speed (WS) at various wind directions

7.5.5 Change in wind direction and vertical dispersion coefficient

Figure 7.19 illustrates that the predicted average concentration at receptor P1 rapidly decreases as the vertical dispersion coefficient increases in all wind directions. In fact, in the wind directions of -1, 45 and 59 degrees, the predicted average concentration is higher than that in wind direction of 29 degrees because in the former the wind tends to flow from the stone processing plants toward to receptor P1.

Figure 7.20 illustrates that the predicted average concentration at receptor P2 substantially drops as the vertical dispersion coefficient increases in all wind directions. In fact the concentration for wind direction of 59 degrees is highest at P2 because the wind direction tends to shift the flow toward to the receptor as it shifts toward 59 degrees.

Similar to receptor P2, the vertical dispersion coefficient shows the same effect on the predicted average concentration at receptor P3 in all wind directions as shown in Figure 7.21. The only major disagreement between the two receptors is the reverse effect of the wind direction on the predicted average concentration at the two receptors.

In Figure 7.22, the vertical dispersion coefficient again has a strongly negative effect on the predicted average concentration at P4 in all wind directions of interest whereas the wind direction seems to have only a small influence because P4 is located behind a hill for all wind directions and the predicted PM_{10} concentration at P4 depends more on the dispersion than the convection mechanism.

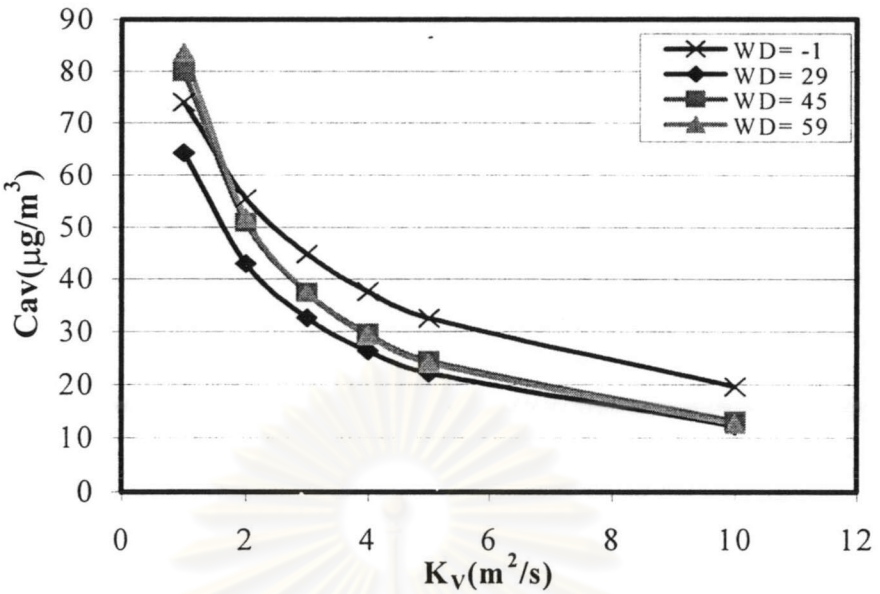

Figure 7.19 The change in the predicted average concentration at Receptor P1 by the change in the vertical dispersion coefficient for various wind directions

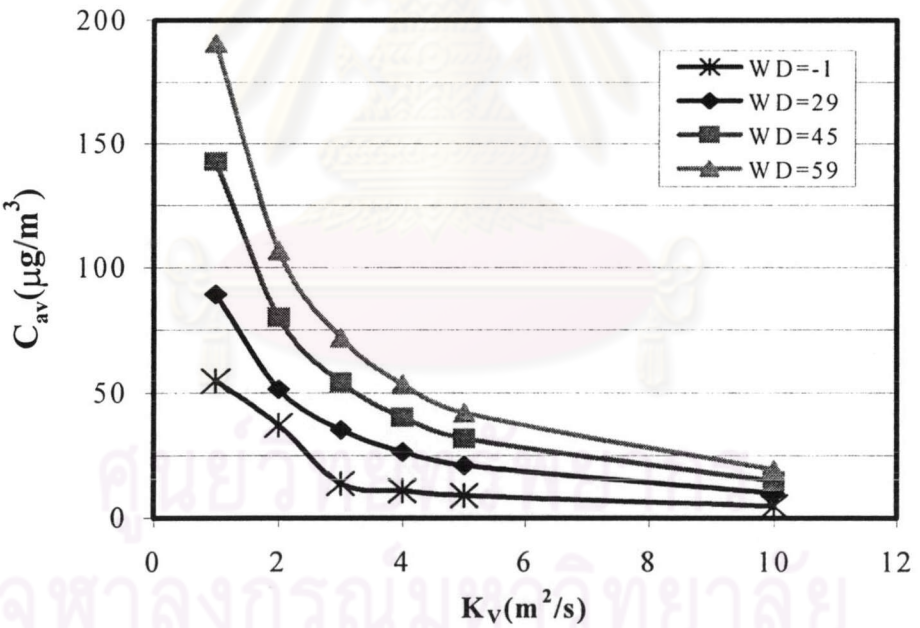

Figure 7.20 The change in the predicted average concentration at Receptor P2 by the change in the vertical dispersion coefficient for various wind directions

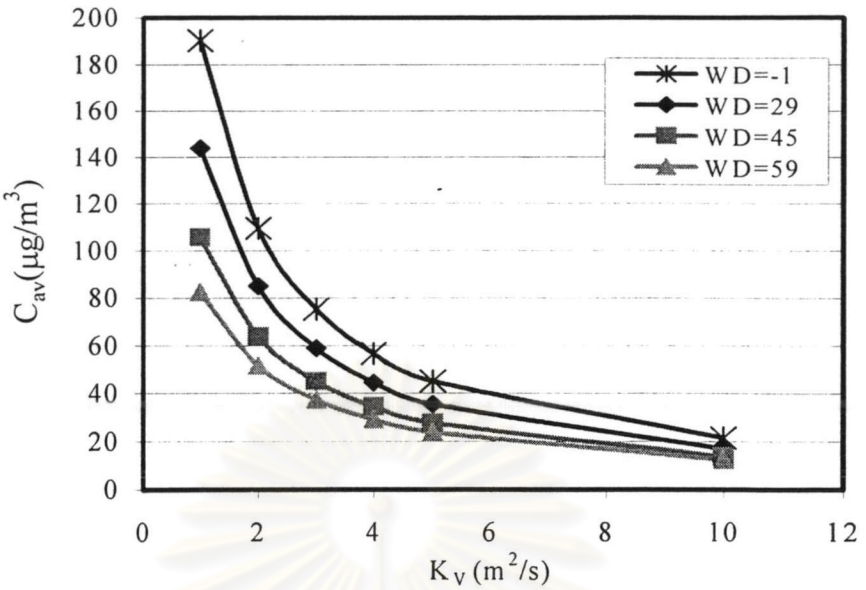

Figure 7.21 The change in the predicted average concentration at Receptor P3 by the change in the vertical dispersion coefficient for various wind directions

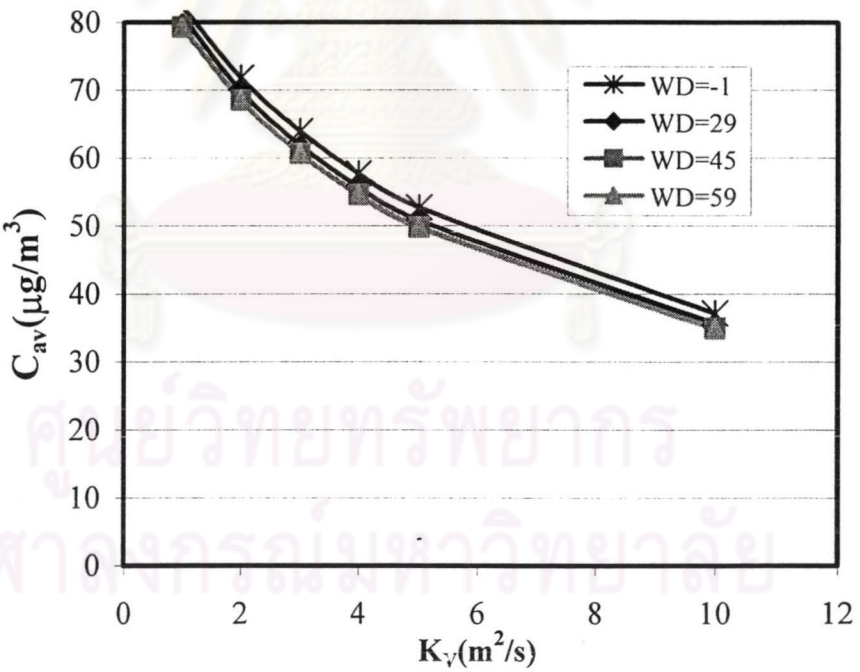

Figure 7.22 The change in the predicted average concentration at Receptor P4 by the change in the vertical dispersion coefficient for various wind directions

7.5.6 Change in wind speed and vertical dispersion coefficient

As shown in Figure 7.23, at all wind speeds the predicted average concentration at receptor P1 decreases as K_V increases but the change in the wind speed hardly has any influence on the predicted concentration. Since the wind direction of 29 degrees does not flow from the source directly toward the receptor, the PM_{10} concentration results from the dispersion rather than convection mechanism. Figure 7.24 illustrates that as the vertical dispersion coefficient increases at wind speeds of 1 m/s and 0.5 m/s the predicted average concentration at receptor P2 rapidly drops whereas at the wind speed of 2 m/s there is little effect on the average concentration. Again the wind direction flows away from the receptor. The vertical dispersion coefficient has no effect at the high wind speed because the convective transport dominates the dispersion phenomenon. As for receptor P3, increasing the vertical dispersion coefficient again dramatically decreases the predicted average concentration at the receptor at all wind speeds shown in Figure 7.25. In addition a higher wind speed has positive effect on PM_{10} concentration, especially under highly stable atmospheric condition (small vertical dispersion coefficient), in which the predicted average concentration at the receptor exceeds the air quality standard of 120 $\mu g/m^3$ at all wind speeds. Figure 7.26 illustrates that the predicted average concentration at receptor P4 gradually decreases as K_V increases or as wind speed increases because the wind does not flow toward the receptor and the receptor is located on the lee side. Consequently, the concentration at the receptor depends on the dispersion more than the convection mechanism.

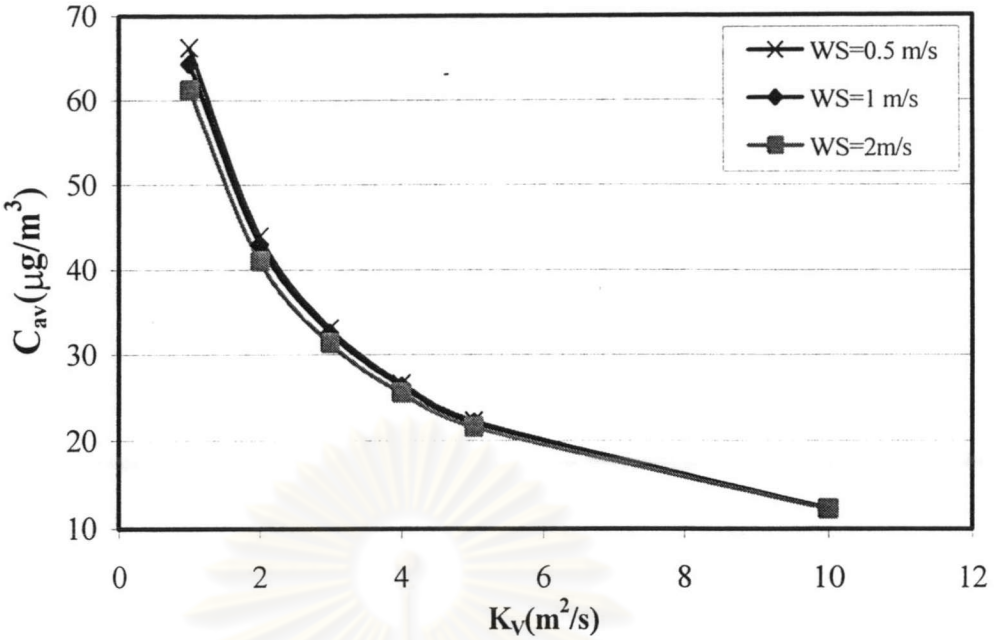

Figure 7.23 The change in the predicted average concentration at Receptor P1 by the change in the vertical dispersion coefficient at various wind speeds (wind direction 29 degrees)

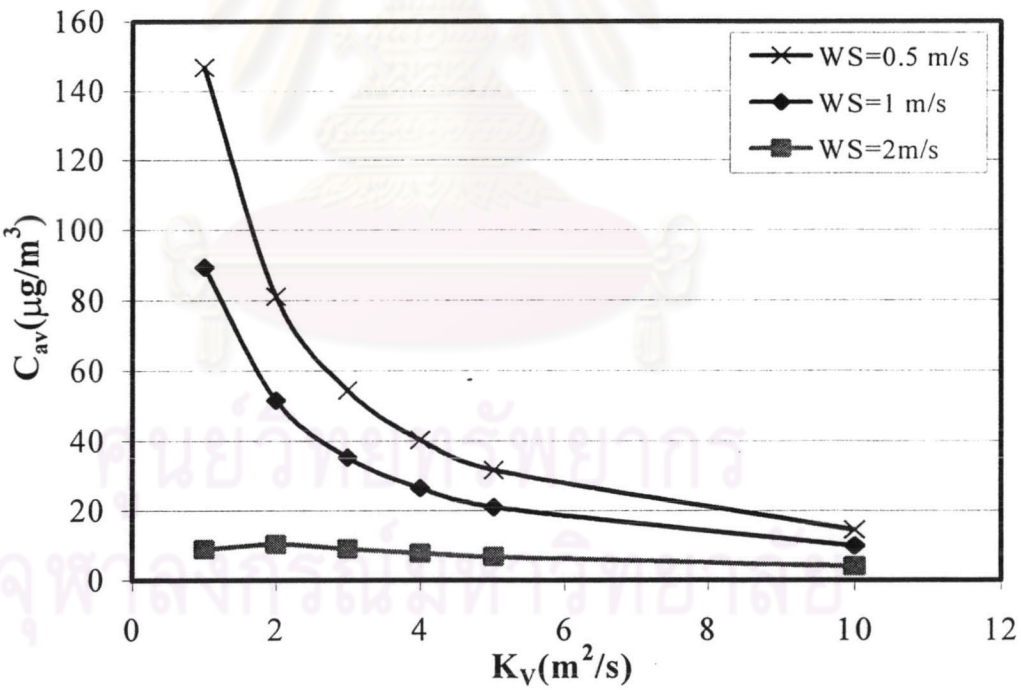

Figure 7.24 The change in the predicted average concentration at Receptor P2 by the change in the vertical dispersion coefficient at various wind speeds (wind direction 29 degrees)

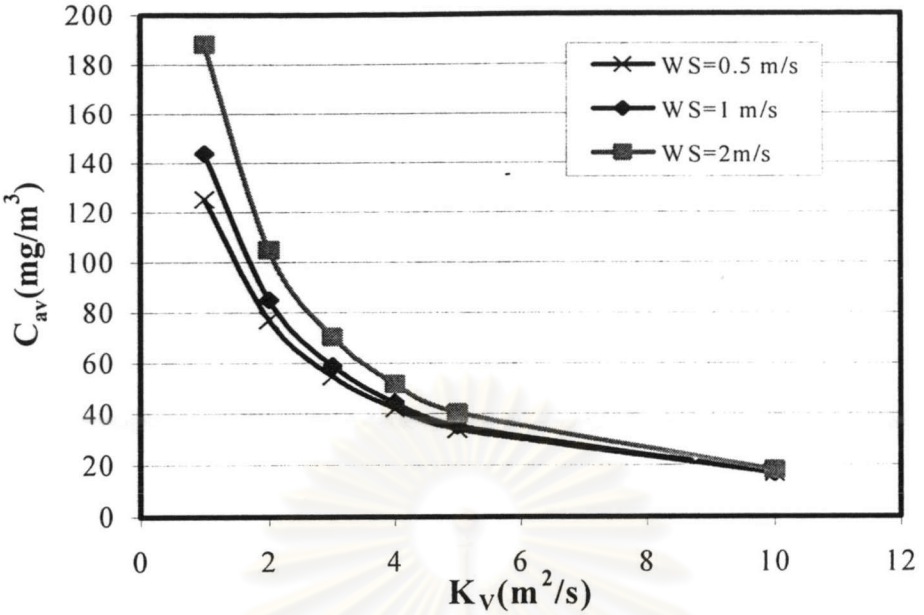

Figure 7.25 The change in the predicted average concentration at Receptor P3 by the change in the vertical dispersion coefficient at various wind speeds (wind direction 29 degrees)

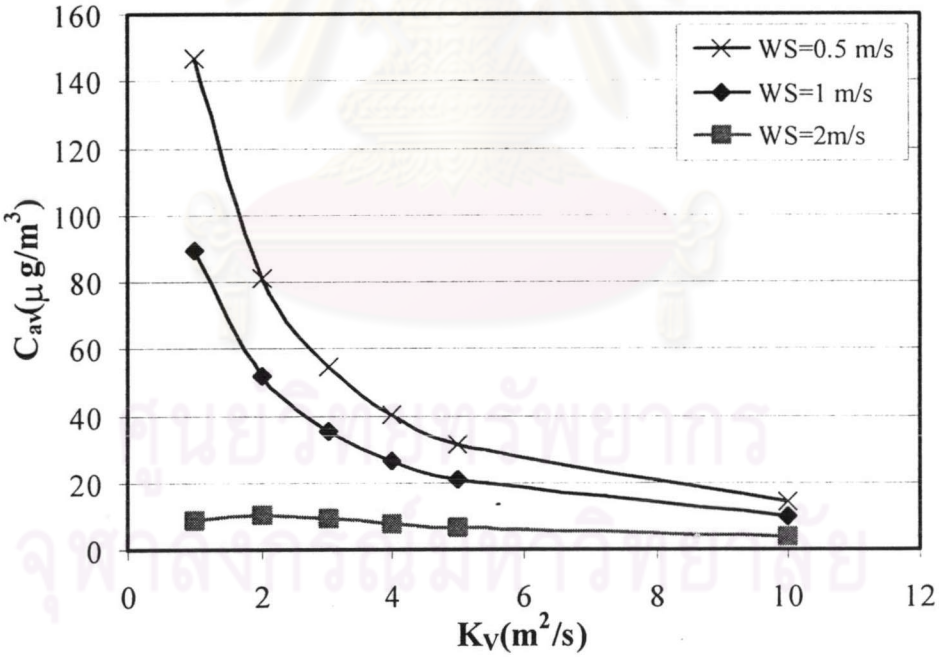

Figure 7.26 The change in the predicted average concentration at Receptor P4 by the change in the vertical dispersion coefficient at various wind speeds (wind direction 29 degrees)2

7.6 Effect of emission factor

In this study, the emission factor (E.F.) used to estimate the dust emission rate of stone crushing plants in the area of interest is 0.05275 kg/ton as shown in Appendix E. Table 7.4 shows that the predicted average concentration is doubled when the emission factor increases by 2 times (E.F.=0.1055) and is halved when the emission factor is reduced by half (E.F.=0.02638). Therefore, it can be concluded that the change in the predicted average concentration is proportional to the emission factor, or more correctly, the emission rate if the plant capacity is also varied.

Table 7.4 The predicted average concentration of PM_{10} at all receptors for various emission factors (E.F.)

Receptor Point	Predicted average concentration ($\mu g/m^3$)		
	E.F.=0.05275	**E.F.=0.02638**	**E.F. = 0.1055**
1	64.3088	32.1544	128.6175
2	89.4632	44.7316	178.9265
3	143.8285	71.9142	287.6570
4	81.0012	40.5006	162.0024
5	0.2200	0.1100	0.440064
6	2.2290	1.1145	4.4581
7	2.0088	1.0044	4.01766
8	194.2690	97.1345	388.5379
9	7.6415	3.8208	15.2831
10	154.7569	77.3785	309.5137
11	0.0000	0.0000	0.0000

In conclusion, when the atmospheric stability increases, the predicted average concentration at all receptors also increases. As for receptor P1, the most significant wind direction lies in the range of 45-59 degrees and the highest wind speed has the most significant effect. In contrast, at receptor P2 the lowest wind speed and the wind direction greater than 59 degrees have the most significant effect. However, the predicted average concentration at receptor P2 nearly exceeds the air quality standard (120 $\mu g/m^3$). The smallest wind direction and the highest wind speed has the most significant effect on the predicted average concentration at receptor P3. Generally the various wind directions do not cause a significant difference in the predicted average concentration at receptor P4 but the low wind speed condition has the most significant effect.

7.7. The Effect of the boundary conditions on the predicted concentration

To prove that the choice of downwind boundary condition (B.C.) made in the previous simulations is appropriate, the simulation results from the previous section are compared with those obtained with a change in the type of downwind boundary conditions.

In case of unchanged B.C., they are as follows:

- $C = 0$, at $x = -\frac{\Delta x}{2}$ (0<z<zmax, 0<y<ymax)

- $C = 0$, at $x = x_{max} + \frac{\Delta x}{2}$ (0<z<zmax, 0<y<ymax)

- $C = 0$, at $z = -\frac{\Delta z}{2}$ (0<x<xmax, 0<y<ymax)

- $C = 0$, at $z = z_{max} + \frac{\Delta z}{2}$ (0<x<xmax, 0<y<ymax)

- C = 0 , at $y = -\frac{\Delta y}{2}$ (0<x<xmax, 0<z<zmax)

- C = 0 , at $y = y_{max} + \frac{\Delta y}{2}$ (0<x<xmax, 0<z<zmax)

In the case of changed downwind B.C., the boundary conditions are as follows:

- C = 0 , at $x = -\frac{\Delta x}{2}$ ($0<z<z_{max}$, $0<y<y_{max}$)

$-\left(\frac{\partial C}{\partial x}\right)_{z,y} = 0$, at $x = x_{max}$ ($0<z<z_{max}$, $0<y<y_{max}$)

- C = 0 , at $z = -\frac{\Delta z}{2}$ ($0<x<x_{max}$, $0<y<y_{max}$)

$-\left(\frac{\partial C}{\partial z}\right)_{x,y} = 0$, at $z = z_{max}$ ($0<x<x_{max}$, $0<y<y_{max}$)

- C = 0 , at $-\frac{\Delta y}{2}$ ($0<x<x_{max}$, $0<z<z_{max}$)

$-\left(\frac{\partial C}{\partial y}\right)_{x,z} = 0$, at $y = y_{max} + \frac{\Delta y}{2}$ ($0<x<x_{max}$, $0<z<z_{max}$)

where C = concentration ($\mu g/m^3$)

From Table 7.5, it can concluded that the change in the type of downwind boundary conditions does not significantly affect the predicted average concentration of PM_{10}.

Table 7.5 The predicted average concentration of PM_{10} at all receptors for the changed and unchanged downwind boundary conditions (B.C.)

Receptor point	Predicted average concentration ($\mu g/m^3$)			
	Wind speed = 2.0m/s		Wind speed = 0.5m/s	
	Unchanged B.C.	Changed B.C.	Unchanged B.C.	Changed B.C.
1	61.2100	61.2100	66.2964	66.2964
2	8.9413	8.9413	146.9094	146.9094
3	188.2658	188.2658	125.3451	125.3451
4	58.1558	58.1558	101.6529	101.6529
5	0.0000	0.0000	0.8103	0.8103
6	0.7445	0.7445	4.0182	4.0182
7	0.0000	0.0000	9.2912	9.2912
8	162.9093	164.8472	207.7812	208.4388
9	5.3353	5.3353	7.6559	7.6559
10	154.2648	154.2648	149.2939	149.2939
11	0.0000	0.0000	0.0234	0.0234